Bioelectrochemistry 122 (2018) 61–68

Contents lists available at ScienceDirect

Bioelectrochemistry

journal homepage: www.elsevier.com/locate/bioelechem

Removal of binary Cr(VI) and Cd(II) from the catholyte of MFCs and determining their fate in EAB using fluorescence probes☆

Liping Huang [a,*], Peng Zhou [b], Xie Quan [a], Bruce E. Logan [c]

[a] Key Laboratory of Industrial Ecology and Environmental Engineering, Ministry of Education (MOE), School of Environmental Science and Technology, Dalian University of Technology, Dalian 116024, China
[b] College of Chemistry, Dalian University of Technology, Dalian 116024, China
[c] Department of Civil and Environmental Engineering, The Pennsylvania State University, University Park, PA 16802, United States

ARTICLE INFO

Article history:
Received 25 January 2018
Received in revised form 13 February 2018
Accepted 28 February 2018
Available online xxxx

Keywords:
Microbial fuel cell
Electrochemically active bacteria
Fluorescence probe
Cr(VI)
Cd(II)

ABSTRACT

Electrochemically active bacteria (EAB) on the cathodes of microbial fuel cells (MFCs) can remove metals from the catholyte, but the fate of metals in the cells has not been examined in the presence of multiple metals. To study the relative uptake and fate of Cr(VI) and Cd(II) in cells, fluorescence probes were used to determine the amount and location of these metals in four different EAB on the biocathodes of MFCs. When both metals were present, less Cr(VI) was removed but Cd(II) uptake was not appreciably affected. As a consequence, the imaging of Cr(III) ions was lower than that using individual fluorescence probes for single Cr(III) ions in each EAB, compared to negligible changes in images for Cd(II) ions in the presence of either both Cr(VI) and Cd(II) or Cd(II) alone. The concentration of Cr(III) ions in the cells consistently increased over time, while that of Cd(II) ions decreased following an initial increase. Cr or Cd uptake could not be detected using a scanning electron microscope coupled with an energy dispersive spectrometer, reflecting the high sensitivities of the fluorescence probes to these metals. More chromium was found in the cytoplasm while cadmium preferentially accumulated in the cell envelope. These results demonstrate that the fate of chromium and cadmium in EAB was different when both metals were present, compared to controls containing a single metal. These results provide direct and visible results on the fate of the metals in the EAB when these metals are co-present in the catholyte of MFCs.

1. Introduction

Bacteria are capable of removing metals to very low concentrations, and thus they have attracted great interest for applications in metals remediation [1,2]. Bacteria that grow on the cathodes of microbial fuel cells (MFCs), called electrochemically active bacteria (EAB), can accept electrons and reduce oxygen or a variety of different metals making it possible to remove metals while simultaneously generating electricity [3–8]. Metals removal by a biocathode is particularly useful for removing toxic Cr(VI) and Cd(II), which are usually both present in a variety of metal-processing wastewaters [1,2,9]. Most studies on these metals have examined only the removal of a single metal from solution despite the presence of both metals in actual wastewaters [6,10–14]. However, for practical bioremediation applications, it is desirable to simultaneously remove both metals from solution.

The fate of Cr(VI) and Cd(II) within the cell has not been well examined, particularly from the perspective of their simultaneous presence in a wastewater. Soluble Cr(VI) can be reduced to Cr(III)-complexes and precipitated $Cr(OH)_3$ via the transiently formed Cr(III) ions, but when Cd(II) is present it can form organic metal-complexes containing or inorganic precipitates containing both metals. These metals can be found on the bacterial outer membranes, or in the cytoplasm or periplasm. Previous studies have examined the uptake of these metals using techniques such as global kinetic analysis and titrimetry [15–17]. The presence of these metals in the cells has been investigated using many different techniques, including X-ray absorption near-edge structure (XANES), extended X-ray absorption fine structure (EXAFS), inductively coupled plasma mass spectroscopy (ICP-MS), low frequency electron spin resonance (ESR) spectrometry, X-ray photoelectron spectroscopy (XPS), raman spectroscopy, scanning electron microscope equipped with energy dispersive spectroscopy (SEM-EDS), and transmission electron microscopy equipped with energy dispersive spectroscopy (TEM-EDS) [18,19]. However, these techniques do not quantify the amount of metal take up, or the locations of transiently formed Cr(III) ions and the permeated Cd(II) ions inside of bacteria. Thus, different techniques are needed to assess the concentration and location of Cr(III) and Cd(II) ions on or in the cells.

Fluorescent probes for metals have recently been shown to be useful as a highly sensitive, rapid, and nondestructive way to visually and quantitatively identify metals in cells [20,21]. These probes have

☆ The authors declare no competing financial interest.
* Corresponding author.
E-mail address: lipinghuang@dlut.edu.cn (L. Huang).

https://doi.org/10.1016/j.bioelechem.2018.02.010
1567-5394/

individually identified Cr(III) [22] or Cd(II) [23] in bacteria, but they have not been simultaneously used to track the location of these metals. In most practical situations both metals are often present, and it is not known how the presence of both these metals might impact the fate of the metals in the cells. Thus, simultaneous imaging sensing of Cr (III) and Cd(II) ions in EAB could reveal whether different amounts of the metals were taken up in the presence of both metals, and show whether the preferential location of these metals might change compared to tests with individual metals. An understanding of the fate of these metals could lead to improvements in the removal effectiveness of bioremediation using biocathodes and other electrochemical processes for in-situ remediation.

In order to quantify the uptake and fate of both Cr(VI) and Cd(II) metals when both metals were present, pure culture MFC experiments were conducted using four known EAB that were isolated from Cr(VI) reducing biocathodes, *Stenotrophomonas* sp. YS1, *Stenotrophomonas maltophilia* YS2, *Serratia marcescens* YS3, and *Achromobacter xylosoxidans* YS8 [22,24]. As controls, the distribution of subcellular chromium in the presence of only Cr(VI) in catholyte and subcellular cadmium in the presence of single Cd(II) in catholyte was also mapped. Using pure culture strains allow us to directly understand the EAB at the electrode surface for Cr(VI) and Cd(II) removal whereas comparing the EAB behaviors is beneficial for understanding the distribution of various valence states of chromium and cadmium in the EAB. A naphthalimide-rhodamine based Cr(III) probe [25] and a quinoline-based Cd(II) probe [26] were simultaneously used to evaluate the uptake and fate of the two metals added alone or together to the cathodes of MFCs with current generation, and compared to open circuit controls or abiotic cathodes. Cr(III) and Cd(II) ions were then identified in the protoplasm and in the cytoplasm of the cells.

2. Materials and methods

2.1. Inoculation and MFC operation

Pure cultures of the four EAB (YS1, YS2, YS3, and YS8) were incubated in an anaerobic medium (AM, pH = 5.8) containing: NH_4Cl (5794 μM), KCl (1743 μM), $MgCl_2 \cdot 6H_2O$ (885 μM), $CaCl_2 \cdot 2H_2O$ (612 μM), KH_2PO_4 (11.0 mM), $K_2HPO_4 \cdot 3H_2O$ (12.7 mM), and 1 mL of trace elements [22].

Duplicate two-chamber MFCs were used in all experiments as previously described [22]. Briefly, porous graphite felt (each piece: 1.0 × 1.0 × 0.5 cm, with a total of 8 pieces; Sanye Co., Beijing, China) was inserted with carbon rod collectors and used for the cathodes and anodes [22,27,28]. The anode (26 mL) and cathode (13 mL) chambers were separated by a cation exchange membrane (CEM) (CMI-7000 Membranes International, Glen Rock, NJ) with a projected surface area of 7.1 cm^2 [29]. The anodes were inoculated using the effluent of MFCs well acclimated to acetate (12.2 mM) [30,31]. The electrolyte in both chambers was AM, except for the catholyte where acetate was replaced by $NaHCO_3$ (119 μM). Solution conductivities were adjusted to be 5.8 mS/cm using 0.1 M KCl [32,33]. Both the anolyte and catholyte were bubbled with ultra-pure N_2 for 10 min, and then sealed in order to maintain anaerobic condition during the experiments. The MFCs were operated at a fixed external resistance of 510 Ω, and a reference electrode (Ag/AgCl, 195 mV vs. SHE) was placed in the cathode chamber to measure the cathode potential. All potentials were reported vs SHE. All reactors were wrapped with aluminum foil to exclude light.

Cathodes were inoculated with one of the four different isolates (6 mL containing 10^8 CFU/mL), and each cycle of MFC operation was set at 5 h. Concentrations of chromium and cadmium in actual wastewaters can vary over a large range of 0.008–5190 mM [2,30,31]. For metal reduction experiments here, Cr(VI) (385 μM) and Cd(II) (179 μM) were added to AM at concentrations within this range, consistent with previous studies on the activities of these microorganisms [14,22,23]. Three replicate experiments were performed with both metals using duplicate reactors with current generation. Three types of reactors (in duplicate) were used as controls: one was operated without the inoculum (abiotic control); the second was inoculated but operated under open circuit conditions (OCC) to examine removal in the absence of current generation; and the third was operated in the presence of only a single metal to contrast changes with two metals with that of Cr(VI) or Cd(II) alone in the system.

2.2. Preparation of Cr(III) and Cd(II) fluorescent probes

The fluorescent probes were synthesized for Cr(III) ions as described by Mao et al. [25], and for Cd(II) ions by Xu et al. [26] (Fig. S1). The chemical properties of the probes were confirmed by high resolution mass spectrum (HRMS) data, and 1H and 13C nuclear magnetic resonance spectra (NMR) as previously described [22,23].

2.3. Assessment of toxicity and selectivity of fluorescence probes

Prior to imaging studies, cell viability in the absence and presence of both fluorescence probes (each at concentrations of 5, 10, 20, 30 μM) was assessed using 96-well plates based on growth in AM. Briefly, EAB grown in AM for 24 h were treated with fluorescent probes and incubated for another 24 h at 30 °C. A FD FACSCanto flow cytometer (Biosciences) was used to assess the viability [22]. Cell survival in the presence of the probes were normalized to the untreated control cells. Experiments were performed at least 3 times.

In order to assess selectivity of the probes, bacteria were first incubated in the absence of Cr(VI) and Cd(II). Cell periplasm and cytoplasm were then prepared through ultrasonic cell disruption, osmotic shock and centrifugation as described in SI [22,23,28] before exposed to the probes and metal ions. The selectivity of Cr(III) and Cd(II) probes toward Cr(III) and Cd(II) ions in the periplasm and cytoplasm samples was examined using either Cr(III) or Cd(II) ions, and then both Cd(II) or Cr(III) ions. Finally, in the presence of both fluorescence probes and Cr(III) and Cd(II) ions, fluorescence intensities were examined before and after adding other individual metal cations [Zn(II), Fe(III), Co(II), Mn(II), Ni(II), Ca(II), K(I), Na(I)]. Standard curves for the responses of Cr(III) or Cd(II) probes to Cr(III) or Cd(II) ions in either the cytoplasm or periplasm of the four bacteria, and detection limits of these probes, were established based on the description of cytoplasm and periplasm preparation in SI. Relative errors ranged from 9 to 17%.

2.4. Imaging of Cr(III) and Cd(II) ions in live cells

Images for Cr(III) and Cd(II) ions in live cells were examined using confocal laser scanning microscopy (CLSM) (Olympus FV 1000, Japan). Briefly, cells were incubated with both probes (10 μM each) at 30 °C for 20 min, rinsed three times by centrifugation (6000 ×g), and re-suspended in saline water (1 mL). A sample (100 μL) was placed on a clean coverslip and covered with agar (3 mL) at 40 °C for 20 min. Cells were then observed using CLSM under 400 × oil-immersion objective lens (Green channel (520–620 nm), λ_{ex} = 488 nm; red channel (420–480 nm), λ_{ex} = 405 nm). Fluorescence microscopy images were normalized to the brightest sample of the entire set using ImageJ software (NIH, Bethesda, MD). Image analysis and fluorescence quantification was conducted according to the procedure of Kellenberger et al. [34] (see details in the SI). The statistical significance ($p \le 0.05$) of differences between samples was assessed using a statistical package (*t*-test, SPSS v.19.0). Two controls were performed: cell suspensions in the absence of fluorescence probes, and addition of the probes in the absence of cells.

2.5. Measurements and analyses

Average current was calculated based on the sum of current for each operation interval divided by entire operation time (5 h). Polarization

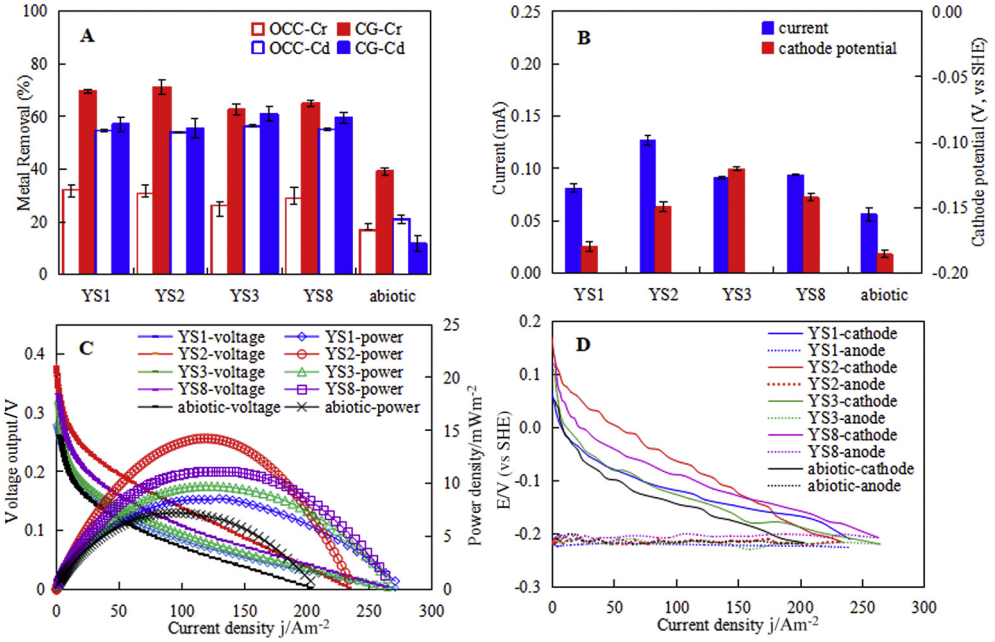

Fig. 1. Metal removals and MFC performance in the presence of both Cr(VI) and Cd(II). (A) Metal removals for Cr(VI) or Cd(II) with current generation (CG) or for open circuit controls (OCC), (B) current and cathode potentials, (C) polarization and power density curves and (D) electrode potentials as a function of current density (operation time of 5 h).

data were obtained with a potentiostat (BioLogic, VSP, France) using linear sweep voltammetry (LSV) at a scan rate of 0.1 mV/s. Power density is often normalized by the electrode projected surface area. In the MFCs used here, both the anodes and cathodes were porous graphite felt with high surface areas, but the separator (or membrane) is known to often limit power production in MFCs [35]. Therefore, power was normalized to the projected surface area of the separator, allowing comparison to previous studies based on power per cross sectional area [35], in addition to providing absolute values with power normalized to the projected surface area of the separator.

Total chromium and cadmium concentrations in solution were determined using an atomic absorption spectrophotometer (AAS, SHIMADZU AA-6300) (detection levels of 0.58 μM (Cr) and 0.01 μM (Cd)), whereas dissolved Cr(VI) was obtained according to standard methods (detection level: 4.0 μM) [36]. Similarly, total chromium, total cadmium and dissolved Cr(VI) in cellular fractions were obtained through AAS or standard methods [36]. Dissolved Cr(III) or Cd(II) ions in cytoplasm and periplasm were quantified based on the fluorescence probe titration experiments. Briefly, periplasmic or cytoplasmic samples were appropriately diluted (2 times), after which 1 mL dilution was added with Cr(III) and Cd(II) probes (each 10 μL) (stock solutions) to reach a sufficient concentration of 100 μM for probe detection [25,26]. These samples were then quantified by fluorescence (Edinburgh F900 fluorescent spectrometer, Edinburgh Co., UK). The distributions of different forms of chromium or cadmium in the EAB, together with total chromium or cadmium on the electrode, in the catholyte and in the

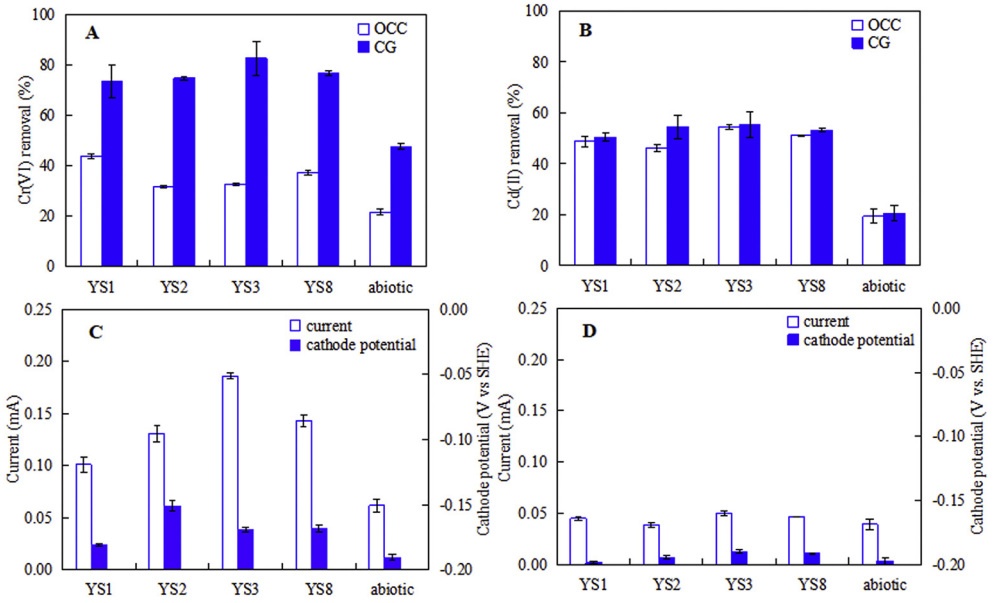

Fig. 2. Metals removals and MFC performance when only a single metal was present. (A) Cr(VI) or (B) Cd(II) removals with current generation (CG) compared to open circuit controls (OCC). Current and cathode potentials for (C) Cr(VI) and (D) Cd(II).

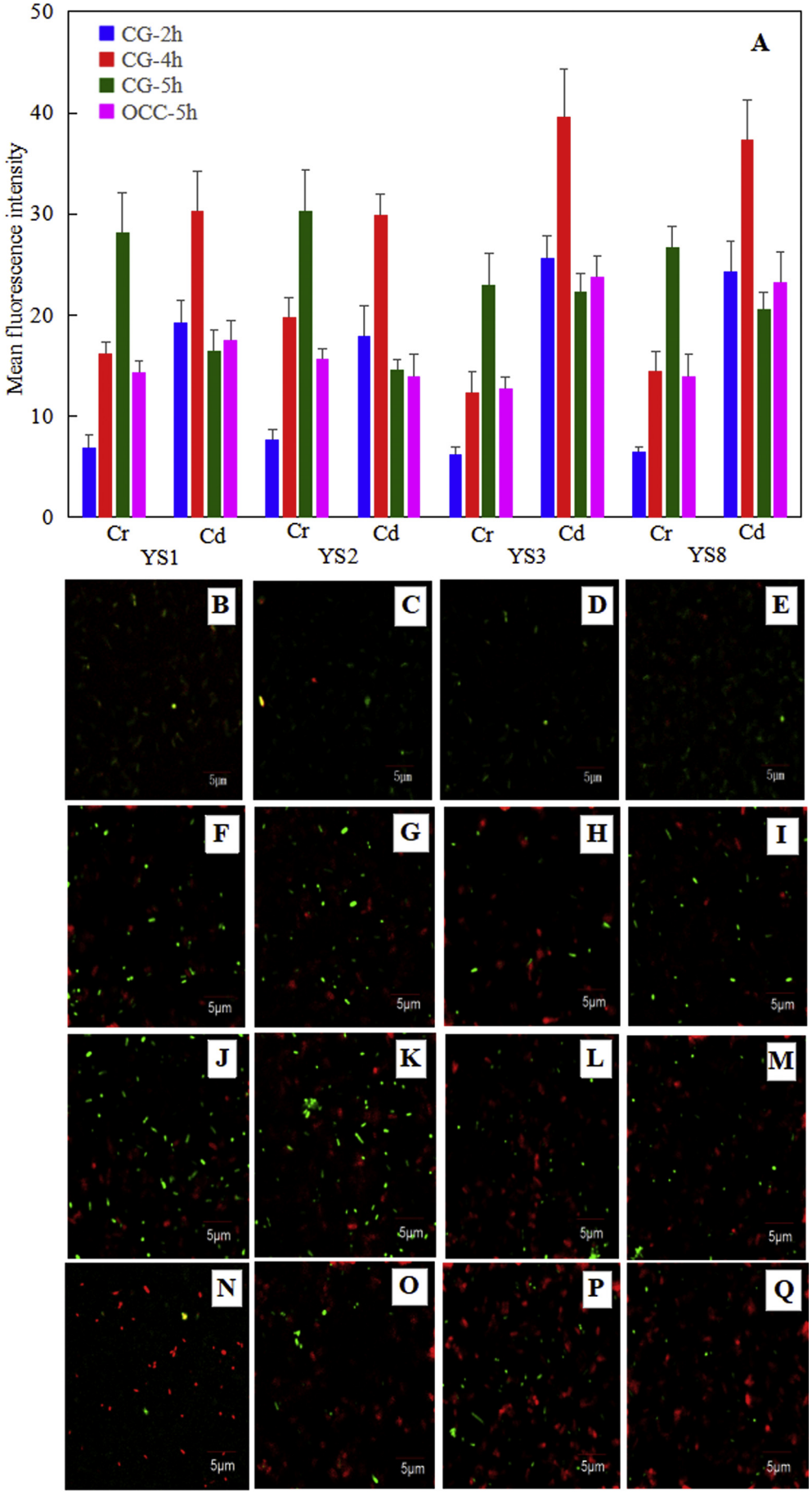
A
CG-2h
CG-4h
CG-5h
OCC-5h
Mean fluorescence intensity
0
10
20
30
40
50
Cr
Cd
YS1
YS2
YS3
YS8
B
C
D
E
F
G
H
I
J
K
L
M
N
O
P
Q
5μm

EAB were normalized by the total initial chromium or cadmium concentrations. All analyses described were conducted in triplicate.

Samples for analysis of the metal concentrations in the membrane, periplasm, or cytoplasm of the cells were first prepared by ultrasonic cell disruption, osmotic shock, and centrifugation as previously reported [22,23,28] and as summarized in the SI. Cell membrane debris was digested with double acid (HNO_3: $HClO_4$ = 10: 1, v/v) before analysis by AAS, and the measured amount of chromium or cadmium was defined as membrane chromium or membrane cadmium. For periplasm and cytoplasm metal content, other forms of chromium or cadmium (chromium/cadmium-organ, chromium/cadmium precipitates, etc.) were obtained based on the differences between total chromium, Cr (VI) and the dissolved Cr(III) ions, or the total cadmium and the dissolved Cd(II) ions.

3. Results and discussion

3.1. Assessment of EAB activities

Cr(VI) removals in the MFCs decreased in the presence of Cd(II) for each of the four different EAB on the cathode, with removals ranging from 71 ± 3% (YS2) to 63 ± 2% (YS3) (Fig. 1A). When Cd(II) was absent, Cr(VI) removals increased with a range of 73 ± 7% (YS1)–82 ± 7% (YS3) (Fig. 2A). In all cases, the presence of the EAB and current generation increased Cr(VI) removal, as removals were much lower for the open circuit (31 ± 2%, YS1; 26 ± 2%, YS3) and abiotic controls (39 ± 1%) (Fig. 1A).

The rate of Cd(II) removal was not impacted by current or the presence of Cr(VI). Cd(II) removals in the presence of Cr(VI) (61 ± 3% for YS3 to 56 ± 4% for YS2) (Fig. 1A) were not significantly different from those obtained with only Cd(II) in catholyte (p = 0.069 to 0.103) (Fig. 2B) or open circuit controls (p = 0.055 to 0.095) (Fig. 1A). However, Cd(II) removal was increased with EAB on the cathode, as these Cd(II) removals were all higher than those of the abiotic controls (metal removals of 12–21%) (Fig. 1A). No chromium or cadmium was detected in the anolyte during one fed-batch cycle operation, consistent with previous reports [29,30]. This may exclude the possibility of metal diffusion from the cathode to the anode although it was possible that some metal was adsorbed onto bacteria in the anode chamber and thus not present in solution.

MFC performance was improved in the presence of the EAB, and under conditions where there was increased metals removals. For example, the current reached a maximum of 0.127 ± 0.005 mA for YS2 with Cr(VI) in the presence of Cd(II), compared to 0.056 ± 0.006 mA for the abiotic control with both metals (Fig. 1B). In the presence of both metals, current and maximum power density (Fig. 1B and C) were lower than those in the presence of Cr(VI) alone (Figs. 2C and S2A), and negligible current and maximum power density were obtained in the absence of Cr(VI) (Figs. 2D and S2B). These changes in current and power demonstrated the negative impact of Cd(II) and positive influence of Cr(VI) on system performance. Open circuit potentials (OCP) and maximum power densities with both metals were all appreciably higher than those of the abiotic controls (Fig. 1C). The highest OCP of 0.361 V and a maximum power density of 14.2 mW/m^2 (10.1 μW) were produced with YS2 (Fig. 1C). This power density was 100% higher than the abiotic controls, and 66% higher than that obtained with YS1 with the same two metals. The power differences were mainly due to biocathodes, as the anode potentials were similar for all tests (Fig. 1D).

The improved performance with Cr(VI) is consistent with the higher driving potential of Cr(VI), compared to Cd(II)($E_{Cr6+/Cr(OH)3}$ = 1.33 V vs. SHE; $E_{Cd2+/Cd}$ = −0.52 V vs. SHE). It is thus speculated that electrons may have been transferred from the cathodes to the EAB, followed by the electron acceptor of Cr(VI), but this mechanism is not yet proven [3,6,37–39]. It has not yet been demonstrated that electron transfer for this metal is coupled to cell respiration, and there are a variety of other possible mechanisms by which cells might catalyze enhanced reduction of Cr(VI) [37–39].

3.2. Toxicity, selectivity and reversibility of fluorescence probe, and establishment of responses of Cr(III) or Cd(II) probes to Cr(III) or Cd(II) ions in cytoplasm or periplasm

Neither of the fluorescent probes resulted in an observable toxic response from the different EAB incubated at doses ranging from 5 μM to 30 μM (Fig. S3). For both probes, there were linear responses of the fluorescence signals with probe concentrations in both cytoplasm and periplasn samples in the presence of both probes (Figs. S4–S7 and Table S1). The detection limits obtained here were 406–423 nM and 132–157 nM in cytoplasm, and 381–404 nM and 97–108 nM in periplasm, when using both probes (S/N = 3) (Table S1). These were much higher than the detection limits previously reported using single fluorescence probes for Cd(II) ions in other EAB (22–46 nM in cytoplasm; 19–31 nM in periplasm) [23]. Based on these results, fluorescence probe concentrations were therefore set at 10 μM for subsequent tests.

In general, there was little impact of other metal ions on fluorescence in the presence of Cr(III) ions (100 μM) and Cd(II) ions (20 μM) in either periplasm or cytoplasm samples (Figs. S8 and S9). An exception was Mg(II) for YS1 and YS2, and Cu(II) and Mn(II) for YS3 and YS8 where some interference was noted for sensing the Cr(III) probe (Fig. S8). In addition, Cu(II), Mn(II) and Mg(II) in cytoplasm negatively influenced the sensing of Cd(II) probe (Fig. S9B, D, F and H). These results showed a reduced sensitivity with the two probes, compared to that with the single Cr(III) or Cd(II) probes in the presence of the same other metals [22,23].

The solution pH over a range of 4.0–10.0 led to negligible changes in fluorescence intensities of these two probes (data not shown), guaranteeing the stability and the satisfactory sensing abilities of the probes for the experimental pH range of 5.8–6.0.

3.3. Fluorescence imaging for EAB over time

Fluorescence intensities over time varied for the two probes. The intensity of the Cr(III) probe always increased from 2 h to 5 h, whereas of the Cd(II) probe increased from 2 h to 4 h but then decreased from 4 to 5 h (Fig. 3B–Q). These trends were consistent with those of the corresponding mean fluorescence intensities over time based on the total of 60 cells randomly selected for each EAB (Fig. 3A). Overlays of fluorescence and bright-field images (Fig. S10) showed that the fluorescence signals were usually localized in the intracellular areas, implying good cell-membrane permeability of these two chemical sensors. In the controls without fluorescence probes, no fluorescence signals were obtained (data not shown). The fluorescence intensities of imaging Cr (III) and Cd(II) ions (Fig. 3) were lower than the controls with Cr(VI) only (Fig. S11) [22] and similar to single Cd(II) (p = 0.076–0.088) (Fig. S12) in the same EAB at 2 h or 4 h. This demonstrated that the imaging of Cr(III) and Cd(II) ions in EAB was different when both metals were present, compared to controls containing a single metal. A plausible explanation for this phenomena is that the alteration of the membrane-protein composition in response to the co-presence of Cr (VI) and Cd(II) could result in decreased permeability of the cell to Cr

Fig. 3. (A) Mean fluorescence intensity of the cells as a function of operation time with current generation (CG), compared with that in open circuit controls (OCC). Error bars indicate standard error of means for at least 60 cells. Fluorescence images of electrochemically active bacteria (EAB) of YSI (B, F, J and N), YS2 (C, G, K and O), YS3 (D, H, L and P), and YS8 (E, I, M and Q) with both Cr(VI) and Cd(II) metals present, at operation times of 2 h (B, C, D and E), 4 h (F, G, H and I), or 5 h (J, K, L and M), compared to OCC (N, O, P and Q) at 5 h (probe concentrations: 10 μM, touch time: 30 min).

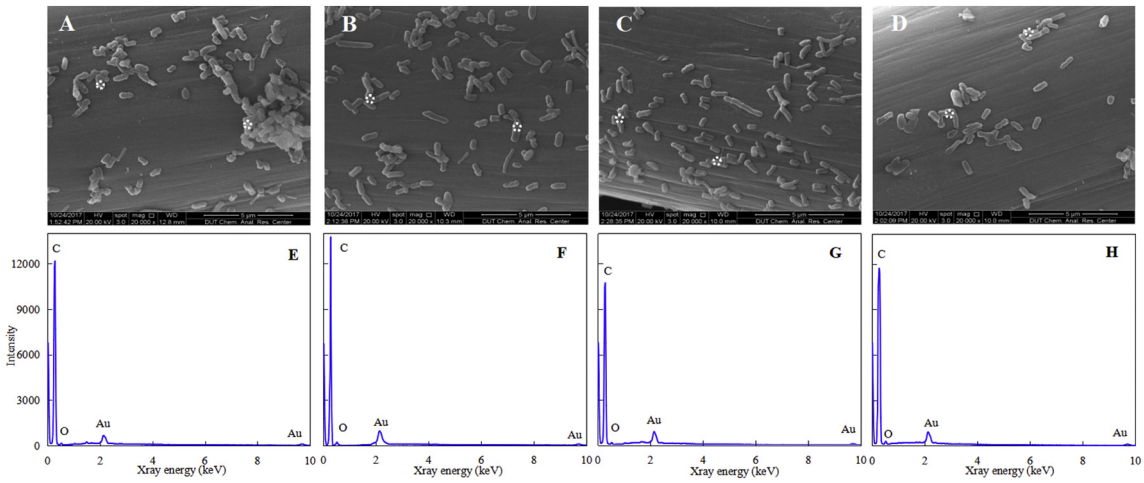

Fig. 4. SEM images (A, B, C and D) and EDS spectra (E, F, G and H) of electrochemically active bacteria (EAB) of YS1 (A and E), YS2 (B and F), YS3 (C and G), and YS8 (D and H) on the cathodes at the end of one fed-batch cycle.

(VI) rather than Cd(II), similar to the observed cadmium and chromium removals by bacterial *Caulobacter crescentus* [40].

3.4. EAB analyzed by SEM-EDS

EAB biofilms were always observed on the cathodes using SEM at the end of the first fed-batch cycle of operation (Fig. 4A, B, C and D). However, no Cr or Cd signals were detected using EDS on the surfaces of these EAB after one cycle (Fig. 4E, F, G and H), illustrating that EDS was not sufficiently sensitive to detectable Cr and Cd compared to the fluorescence probes at the initial low levels. After five cycles, however, both Cr and Cd had accumulated to sufficient levels to enable their detection using EDS (Fig. S13). These results clearly reflected the higher sensitivities of the fluorescence probes to these metal ions than EDS.

3.5. Subcellular distribution of chromium and cadmium in EAB and cathode chamber

Chromium accumulation was consistently higher in the cells (Fig. 5A) than cadmium in the cytoplasm (Fig. 5B). For example,

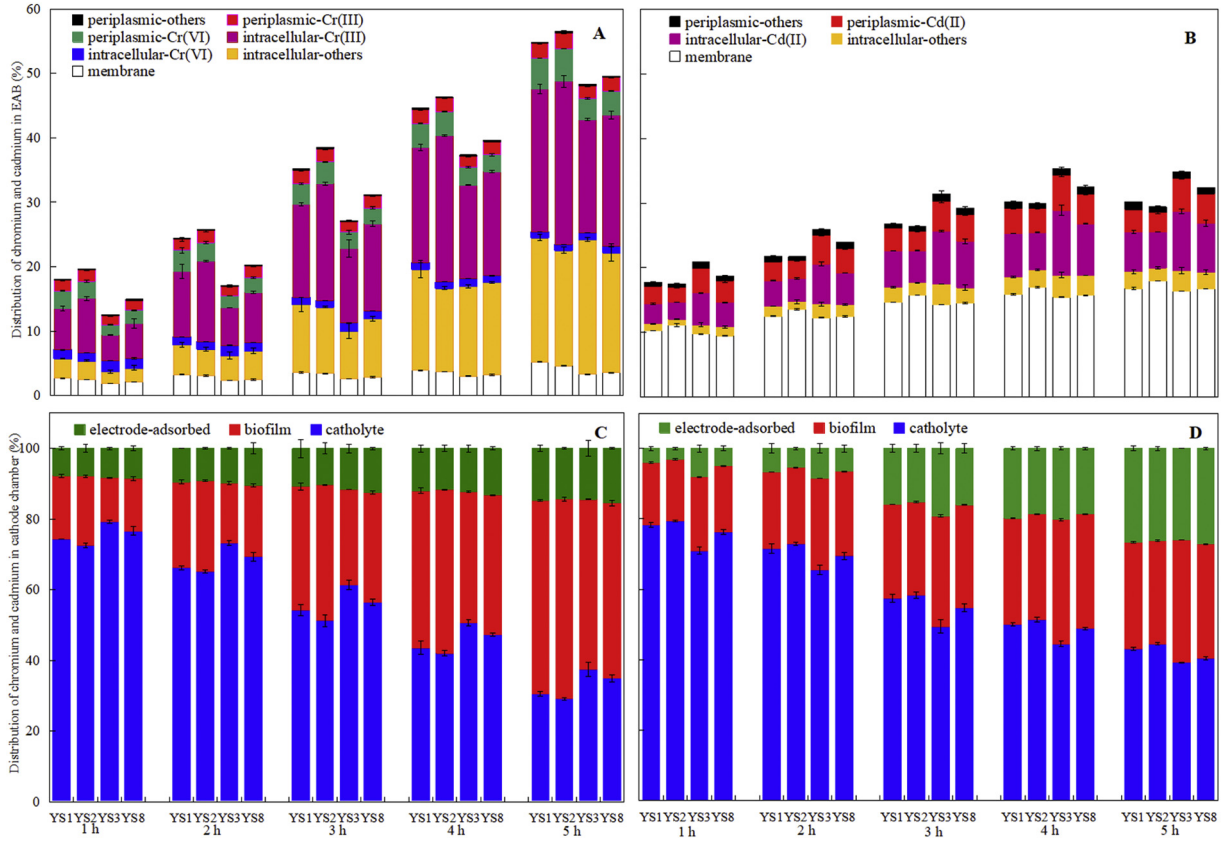

Fig. 5. Distribution of (A) Cr(III) or Cr (VI) in the intracellular or periplasmic fractions, or on the cell membrane, or other forms of chromium (such as precipitates or complexes). (B) Cd(II) in the intracellular or periplasmic fractions, or on the cell membrane, or other forms of cadmium (such as precipitates or complex). Measured concentrations of (C) chromium and (D) cadmium in the catholyte or in the biofilm, with the balance (based on the mass added) assumed to be adsorbed to the electrode (electrode-adsorbed).

intracellular Cr(III) ions reached 4.0 ± 0.1% (YS3) – 8.4 ± 0.3% (YS2) at 1 h and 17.5 ± 0.2% (YS3) – 25.3 ± 0.9% (YS2) at 5 h (Fig. 5A), compared to intracellular Cd(II) ions of 2.7 ± 0.0% (YS2) – 5.0 ± 0.1% (YS3) and 5.5 ± 0.0% (YS2) – 9.2 ± 0.3% (YS3) at the same operation times (Fig. 5B). Similarly, the other forms of chromium in cytoplasm (1.9 ± 0.3% (YS3) – 3.0 ± 0.1% (YS1) at 1 h; 18.0 ± 0.5% (YS2) – 20.9 ± 0.3% (YS3) at 5 h) (Fig. 5A) were also appreciably higher than those of cadmium (1.0 ± 0.1% (YS2) – 1.4 ± 0.3% (YS3) at 1 h; 2.0 ± 0.2% (YS2) – 3.1 ± 0.5% (YS3) at 5 h) (Fig. 5B). These results demonstrated the more preferential chromium accumulation in the presence of both metals. The trends of intracellular Cr(III) (Fig. 5A) and Cd(II) (Fig. 5B) ions were consistent with the imaging of Cr(III) and Cd(II) ions in EAB (Fig. 3A), as there was always an increase of intracellular Cr(III) ions over time, and there was an initial increase of intracellular Cd(II) ions followed by a decrease after 4 h. The cell surfaces harbored appreciably higher cadmium (Fig. 5B) than chromium (Fig. 5A), which was different than that observed for cytoplasm samples. The total accumulated chromium in EAB (Fig. 5A) with current generation (CG) was appreciably higher than that of the OCC (Fig. S14A), but there were negligible changes of cadmium in the presence or absence of current (Fig. 5B and Fig. S14B), consistent with the results in Fig. 1A. These results in concert demonstrated that the fate of chromium and cadmium in EAB was different when both metals were present, compared to controls containing a single metal.

Total chromium in the catholyte decreased over time (Fig. 5C). As the chromium was removed from solution, the amount of chromium in the biofilm increased over time (Fig. 5C). The remaining chromium (based on the difference between the amount added and that detected) was assumed to be adsorbed to the electrode. In all cases, the amount of chromium remaining in the catholyte was less than that remaining in the catholyte of the OCC reactors (Fig. S14C). For cadmium, however, the results with (CG) and without current generation (OCC) resulted in similar concentrations of the metals in the catholyte and biofilm, and on the electrode (Figs. 5D and S14D). This result showed that cadmium uptake was not linked to current generation, consistent with the results in Fig. 1A.

3.6. Implications

These findings show that the fate of chromium and cadmium in EAB was different when both metals were present, compared to controls containing a single metal. The amount of Cr(III) ions and other forms of chromium was invariably higher than Cd(II) ions and other forms of cadmium in the same EAB cytoplasm, and cell envelopes contained more cadmium than chromium. The presence of current increased chromium uptake, but negligibly affected cadmium in all four EAB. These results contributed new insights and an in-depth understanding of the fate of binary Cr(VI) and Cd(II) in EAB, and thus advanced our understanding of biocathode remediation for Cr(VI) and Cd(II) co-contaminant sites. This is of particular importance as biocathodes have been regarded as an alternative approach for heavy metal polluted sites remediation [6,8,24,33].

Two metal fluorescence probes were simultaneously used for the first time, enabling tracking the both binary Cr(III) and Cd(II) ions, and determination of the subsequent distributions of chromium and cadmium inside the cells. This approach allowed the direct and simultaneous sensing of both Cr(III) and Cd(II) ions in these living bacteria, which has not been achieved using other methods [17–21], and it therefore broadens practical applications of fluorescence probes. For the four different EAB, similar trends were observed over time in terms of metal ions and metal distribution based on our fluorescence imaging, despite differences in quantitative amounts. This showed the potential application of this simultaneous two fluorescence probes technology for determining metals in mixed culture since real wastewater commonly contains many different types of bacteria [4,5,7,41–43]. In particular, this approach provides critical insights at the subcellular level which is needed to understand the fate of these metals for practical applications of metals recovery and contaminated-site remediation using bioelectrochemical approaches [6].

Notably, practical implementation of the fluorescence probes for the sensing of Cr(III) and Cd(II) ions in EAB requires to evaluate the applicability of fluorescence probes on EAB over a feed with fluctuating characteristics. In terms of mixed cultures in actual wastewaters, the applicability of the fluorescence probes in a more diverse bacterial community should be further examined. In addition, process economics based on pilot and full-scale MFCs for practical mixed metal wastewater treatment along with the sensing of the fluorescence probes for metal ions in EAB are needed to raise the technology readiness level for industrial applications.

4. Conclusions

EAB removals of both Cr(VI) and Cd(II) from the catholyte with the sensing of imaging binary Cr(III) and Cd(II) ions through fluorescence probes were achieved in this study. Compared to the presence of single Cr(VI) or Cd(II), less Cr(VI) was removed but Cd(II) uptake was not appreciably impacted. As a consequence, the fluorescence intensity of Cr (III) ions in the images with both ions was lower than that using individual fluorescence probe for single Cr(III) ions for each of the EAB, compared to the negligible changes in fluorescence for Cd(II) ions in the presence of either binary Cr(VI) and Cd(II) or single Cd(II) in the catholyte. More chromium was found in the cytoplasm, while cadmium was preferentially accumulated in the cell envelope. These results demonstrated that the fate of chromium and cadmium in EAB was different when both metals were present, compared to controls containing a single metal. This study provides a viable approach for simultaneously tracking binary Cr(III) and Cd(II) ions in EAB using a direct imaging technique, and thus it provides valuable insights into the fate of these metals in different cellular components involved in the immobilization of Cr(VI) and Cd(II) using MFCs.

Acknowledgements

The authors gratefully acknowledge financial support from the Natural Science Foundation of China (Nos. 21777017, 21377019 and 51578104), and the Programme of Introducing Talents of Discipline to Universities (B13012).

Appendix A. Supplementary data

Supplementary data to this article can be found online at https://doi.org/10.1016/j.bioelechem.2018.02.010.

References

[1] M. He, X. Li, H. Liu, S.J. Miller, G. Wang, C. Rensing, Characterization and genomic analysis of a highly chromate resistant and reducing bacterial strain *Lysinibacillus fusiformis* ZC1, J. Hazard. Mater. 185 (2011) 682–688.
[2] M. Wang, Q. Tan, J.F. Chiang, J. Li, Recovery of rare and precious metals from urban mines-a review, Front. Environ. Sci. Eng. 11 (2017) 1.
[3] S. Venkata Mohan, G. Velvizhi, J. Annie Modestra, S. Srikanth, Microbial fuel cell: critical factors regulating bio-catalyzed electrochemical process and recent advancements, Renew. Sust. Energ. Rev. 40 (2014) 779–797.
[4] J. Wu, W. Chen, Y. Yan, K. Gao, C. Liao, Q. Li, X. Wang, Enhanced oxygen reducing biocathode electroactivity by using sediment extract as inoculum, Bioelectrochemistry 117 (2017) 9–14.
[5] L. Rago, P. Cristiani, F. Villa, S. Zecchin, A. Colombo, L. Cavalca, A. Schievano, Influences of dissolved oxygen concentration on biocathodic microbial communities in microbial fuel cells, Bioelectrochemistry 116 (2017) 39–51.
[6] Y.V. Nancharaiah, S. Venkata Mohan, P.N.L. Lens, Biological and bioelectrochemical recovery of critical and scarce metals, Trends Biotechnol. 34 (2016) 137–155.
[7] S.M. Iskander, B. Brazil, J.T. Novak, Z. He, Resource recovery from landfill leachate using bioelectrochemical systems: opportunities, challenges, and perspectives, Bioresour. Technol. 201 (2016) 347–354.
[8] J. Shen, L. Huang, P. Zhou, X. Quan, G. Li Puma, Correlation between circuital current, Cu(II) reduction and cellular electron transfer in EAB isolated from Cu(II)-reduced biocathodes of microbial fuel cells, Bioelectrochemistry 114 (2017) 1–7.

[9] M.W. Luczak, A. Zhitkovich, Role of direct reactivity with metals in chemoprotection by N-acetylcysteine against chromium(VI), cadmium(II) and cobalt(II), Free Radic. Biol. Med. 65 (2013) 262–269.
[10] M. Tandukar, S.J. Huber, T. Onodera, S.G. Pavlostathis, Biological chromium (VI) reduction in the cathode of a microbial fuel cell, Environ. Sci. Technol. 43 (2009) 8159–8165.
[11] L. Huang, X. Chai, G. Chen, B.E. Logan, Effect of set potential on hexavalent chromium reduction and electricity generation from biocathode microbial fuel cells, Environ. Sci. Technol. 45 (2011) 5025–5031.
[12] L. Huang, X. Chai, S. Cheng, G. Chen, Evaluation of carbon-based materials in tubular biocathode microbial fuel cells in terms of hexavalent chromium reduction and electricity generation, Chem. Eng. J. 166 (2011) 652–661.
[13] N. Xafenias, Y. Zhang, C.J. Banks, Enhanced performance of hexavalent chromium reducing cathodes in the presence of *Shewanella oneidensis* MR-1 and lactate, Environ. Sci. Technol. 47 (2013) 4512–4520.
[14] Y. Chen, J. Shen, L. Huang, Y. Pan, X. Quan, Enhanced Cd(II) removal with simultaneous hydrogen production in biocathode microbial electrolysis cells in the presence of acetate or $NaHCO_3$, Int. J. Hydrog. Energy 41 (2016) 13368–13379.
[15] T.L. Kalabegishvili, N.Y. Tsibakhashvili, H.Y.N. Holman, Electron spin resonance study of chromium(V) formation and decomposition by basalt-inhabiting bacteria, Environ. Sci. Technol. 37 (2003) 4678–4684.
[16] G.J. Puzon, A.G. Roberts, D.M. Kramer, L. Xun, Formation of soluble organo-chromium(III) complexes after chromate reduction in the presence of cellular organics, Environ. Sci. Technol. 39 (2005) 2811–2817.
[17] R. Bencheikh-Latmani, A. Obraztsova, M.R. Mackey, M.H. Ellisman, B.M. Tebo, Toxicity of Cr(III) to *Shewanella* sp. strain MR-4 during Cr(VI) reduction, Environ. Sci. Technol. 41 (2007) 214–220.
[18] Y. Wang, P.C. Sevinc, S.M. Belchik, J. Fredrickson, L. Shi, H.P. Lu, Single-cell imaging and spectroscopic analyses of Cr(VI) reduction on the surface of bacterial cells, Langmuir 29 (2013) 950–956.
[19] S. Wu, X. Zhang, Y. Sun, Z. Wu, T. Li, Y. Hu, D. Su, J. Lv, G. Li, Z. Zhang, L. Zheng, J. Zhang, B. Chen, Transformation and immobilization of chromium by *Arbuscular Mycorrhizal* fungi as revealed by SEM–EDS, TEM–EDS, and XAFS, Environ. Sci. Technol. 49 (2015) 14036–14047.
[20] J. Fan, M. Hu, P. Zhan, X. Peng, Energy transfer cassettes based on organic fluorophores: construction and applications in ratiometric sensing, Chem. Soc. Rev. 42 (2013) 29–43.
[21] Y. Yang, Q. Zhao, W. Feng, F. Li, Luminescent chemodosimeters for bioimaging, Chem. Rev. 113 (2013) 192–270.
[22] H. Xue, P. Zhou, L. Huang, X. Quan, J. Yuan, Cathodic Cr(VI) reduction by electrochemically active bacteria sensed by fluorescent probe, Sensors Actuators B Chem. 243 (2017) 303–310.
[23] L. Huang, H. Xue, Q. Zhou, P. Zhou, X. Quan, Imaging and distribution of Cd(II) ions in electrotrophs and its response to current and electron transfer inhibitor in microbial electrolysis cells, Sensors Actuators B Chem. 255 (2018) 244–254.
[24] L. Huang, Q. Wang, L. Jiang, P. Zhou, X. Quan, B.E. Logan, Adaptively evolving bacterial communities for complete and selective reduction of Cr(VI), Cu(II) and Cd(II) in biocathode bioelectrochemical systems, Environ. Sci. Technol. 49 (2015) 9914–9924.
[25] J. Mao, L. Wang, W. Dou, X. Tang, Y. Yan, W. Liu, Tuning the selectivity of two chemosensors to Fe(III) and Cr(III), Org. Lett. 9 (2007) 4567–4570.
[26] L. Xu, M.L. He, H.B. Yang, X. Qian, A simple fluorescent probe for Cd^{2+} in aqueous solution with high selectivity and sensitivity, Dalton Trans. 42 (2013) 8218–8222.
[27] L. Huang, Q. Wang, X. Quan, Y. Liu, G. Chen, Bioanodes/biocathodes formed at optimal potentials enhance subsequent pentachlorophenol degradation and power generation from microbial fuel cells, Bioelectrochemistry 94 (2013) 13–22.
[28] Y. Tao, H. Xue, L. Huang, P. Zhou, W. Yang, X. Quan, J. Yuan, Fluorescent probe based subcellular distribution of Cu(II) ions in living electrotrophs isolated from Cu(II)-reduced biocathodes of microbial fuel cells, Bioresour. Technol. 225 (2017) 316–325.
[29] Y. Qian, L. Huang, Y. Pan, X. Quan, H. Lian, J. Yang, Dependency of migration and reduction of mixed $Cr_2O_7^{2-}$, Cu^{2+} and Cd^{2+} on electric field, ion exchange membrane and metal concentration in microbial fuel cells, Sep. Purif. Technol. 192 (2018) 78–87.
[30] Q. Wang, L. Huang, Y. Pan, P. Zhou, X. Quan, B.E. Logan, H. Chen, Cooperative cathode electrode and in situ deposited copper for subsequent enhanced Cd(II) removal and hydrogen evolution in bioelectrochemical systems, Bioresour. Technol. 200 (2016) 565–571.
[31] Q. Wang, L. Huang, Y. Pan, X. Quan, G. Li Puma, Impact of Fe(III) as an effective mediator for enhanced Cr(VI) reduction in microbial fuel cells: reduction of diffusional resistances and cathode overpotentials, J. Hazard. Mater. 321 (2017) 896–906.
[32] L. Huang, Y. Liu, L. Yu, X. Quan, G. Chen, A new clean approach for production of cobalt dihydroxide from aqueous Co(II) using oxygen-reducing biocathode microbial fuel cells, J. Clean. Prod. 86 (2015) 441–446.
[33] L. Huang, L. Jiang, Q. Wang, X. Quan, J. Yang, L. Chen, Cobalt recovery with simultaneous methane and acetate production in biocathode microbial electrolysis cells, Chem. Eng. J. 253 (2014) 281–290.
[34] C.A. Kellenberger, S.C. Wilson, J. Sales-Lee, M.C. Hammond, RNA-based fluorescent biosensors for live cell imaging of second messengers cyclic di-GMP and cyclic AMP-GMP, J. Am. Chem. Soc. 135 (2013) 4906–4909.
[35] W. Li, G. Sheng, X. Liu, H. Yu, Recent advances in the separators for microial fuel cells, Bioresour. Technol. 102 (2011) 244–252.
[36] American Public Health Association, American Water Works Association, Water Pollution Control Federation, Standard Methods for the Examination of Water and Wastewater, 20th edn American Public Health Association, Washington, 1998.
[37] L. Jourdin, S. Freguia, B.C. Donose, J. Keller, Autotrophic hydrogen-producing biofilm growth sustainable by a cathode as the sole electron and energy source, Bioelectrochemistry 102 (2015) 56–63.
[38] C. Rojas, I.T. Vargas, M. Ann Bruns, J.M. Regan, Electrochemically active microorganisms from an acid mine drainage-affected site promote cathode oxidation in microbial fuel cells, Bioelectrochemistry 118 (2017) 139–146.
[39] L. Shi, H. Dong, G. Reguera, H. Beyenal, A. Lu, J. Liu, H. Yu, K.F. Fredrickson, Extracellular electron transfer mechanisms between microorganisms and minerals, Nat. Rev. Microbiol. 14 (2016) 651–662.
[40] M.C. Yung, J. Ma, M.R. Salemi, B.S. Phinney, G.R. Bowman, Y. Jiao, Shotgun proteomic analysis unveils survival and detoxification strategies by *Caulobacter crescentus* during exposure to uranium, chromium, and cadmium, J. Proteome Res. 13 (2014) 1833–1847.
[41] X. Sheng, R. Liu, X. Song, L. Chen, K. Tomoki, Comparative study on microbial community in intermittently aerated sequencing batch reactors (SBR) and a traditional SBR treating digested piggery wastewater, Front. Environ. Sci. Eng. 11 (2017) 8.
[42] X. Mei, D. Xing, Y. Yang, Q. Liu, H. Zhou, C. Guo, N. Ren, Adaptation of microbial community of the anode biofilm in microbial fuel cells to temperature, Bioelectrochemistry 117 (2017) 29–33.
[43] M. Rimboud, M. Barakat, A. Bergel, B. Erable, Different methods used to form oxygen reducing biocathodes lead to different biomass quantities, bacterial communities, and electrochemical kinetics, Bioelectrochemistry 116 (2017) 24–32.